



Poly(Pentafluorophenyl Methacrylate)-Based Nano-Objects Developed by Photo-PISA as Scaffolds for Post-Polymerization Functionalization

Benoit Couturaud, Panagiotis G. Georgiou, Spyridon Varlas, Joseph R. Jones, Maria C. Arno, Jeffrey C. Foster, and Rachel K. O'Reilly*

The preparation of a functional fluorine-containing block copolymer using reversible addition–fragmentation chain-transfer dispersion polymerization in DMSO as a “platform/scaffold” is explored. The nanostructures, comprised of poly(ethyleneglycol)-*b*-poly(pentafluorophenyl methacrylate) or PEG-*b*-P(PFMA), are formulated via photo-initiated polymerization-induced self-assembly (PISA) followed by post-polymerization modification using different primary amines. A combination of light scattering and microscopy techniques are used to characterize the resulting morphologies. It is found that upon varying the degree of polymerization of the core-forming block of PFMA, only uniform spheres (with textured surfaces) are obtained. These nanostructures are subsequently modified by cross-linking using a non-responsive and a redox-responsive diamine, thus imparting stability to the particles in water. In response to intracellular glutathione (GSH) concentration, destabilization of the micelles occurs as evidenced by dynamic light scattering. The well-defined size, inherent reactivity of the nanoparticles toward nucleophiles, and GSH-responsiveness of the nanospheres make them ideal scaffolds for drug delivery to intracellular compartments with reductive environments.

Polymer-based stimuli-responsive materials have been the subject of significant and sustained research owing to their potential for a range of applications, for example, drug delivery, sensing, smart coatings.^[1] Much effort has been devoted to the development of systems that are responsive to biological changes such as pH,^[2,3] temperature,^[4] redox activity,^[5–9] or enzyme levels.^[10–12] For this purpose, thiol-disulfide chemistry is of considerable interest, as it confers covalent stabilization of structures through reversible cross-linking. Furthermore,

elevated glutathione (GSH) concentration in the intracellular compartments can disassemble disulfide cross-linked nano-particles. These properties make disulfide cross-linked particles highly interesting scaffolds for the delivery of therapeutics into target cells.^[13]

Polymerization-induced self-assembly (PISA) via reversible addition–fragmentation chain-transfer (RAFT) polymerization has emerged as a promising technique for the preparation of polymer assemblies, under dispersion or emulsion polymerization conditions, with controlled sizes and morphologies.^[14] A wide range of “nano-objects,” including spherical micelles, worm-like micelles and vesicles, can be efficiently prepared by in situ chain-extension of the solvophilic macro-chain transfer agent (macro-CTA) with a solvophobic block in either polar or non-polar solvents at high solids content (up to 50% w/w).^[15,16]

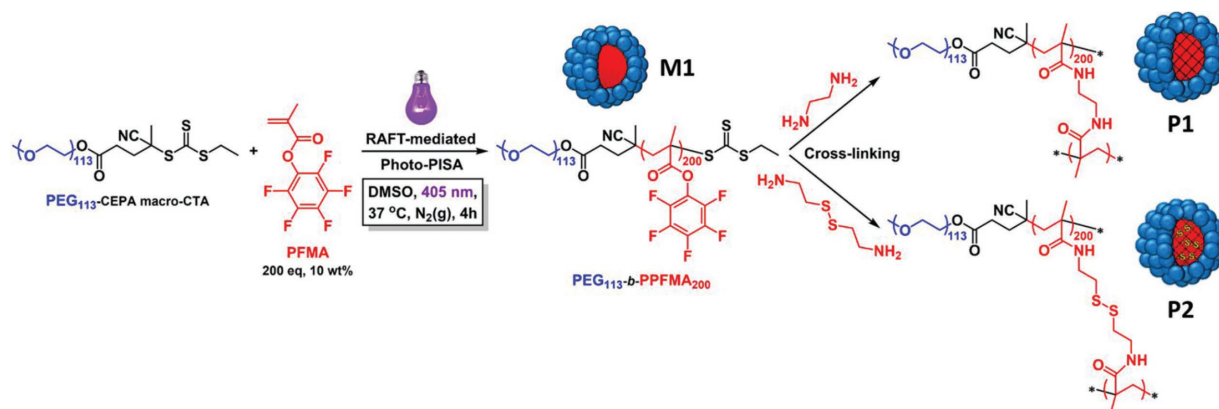
Despite its robustness and versatility, PISA is limited by the fact that only a relatively small class of core-forming monomers and solvents have been reported so far. As a result, the discovery of new monomers and solvents suitable for PISA is of great interest. Recent reports have focused on using (semi)fluorinated methacrylates for RAFT PISA dispersion polymerizations.^[17–21] Fluorinated (or semifluorinated) methacrylates have many interesting properties such as low refractive index and intrinsic hydrophobicity with applications in ¹⁹F-NMR imaging and coatings.^[22–24] In addition, based on the length of the side-chain of the monomers, fluorinated methacrylate-derived polymers have tuneable hydrophilicity. Notably, fluorinated methacrylate monomers are soluble in organic solvents, such as alcohols and toluene, while their corresponding polymers are not. As such, these conditions meet the criteria of the monomers to undergo PISA.^[18] Pentafluorophenyl methacrylate (PFMA) is an activated ester monomer developed and studied extensively by Theato and co-workers.^[25–29] PFMA-based polymers have been extensively used to react with functional amine compounds and to introduce functional side-groups into linear polymer molecules with high yield.^[30,31] Furthermore, a few examples on self-assembly behavior of PPFMA blocks have also been reported.^[32–35] In this work, the PFMA activated esters have been reacted with

Dr. B. Couturaud, P. G. Georgiou, S. Varlas, Dr. J. R. Jones,
Dr. M. C. Arno, Dr. J. C. Foster, Prof. R. K. O'Reilly
School of Chemistry
University of Birmingham
Edgbaston, B15 2TT, Birmingham, UK
E-mail: R.O'Reilly@bham.ac.uk

P. G. Georgiou
Department of Chemistry
University of Warwick
Gibbet Hill Road, CV4 7AL, Coventry, UK

The ORCID identification number(s) for the author(s) of this article can be found under <https://doi.org/10.1002/marc.201800460>.

DOI: 10.1002/marc.201800460



Scheme 1. Schematic illustration of the preparation of poly(ethylene glycol)₁₁₃-*b*-poly(pentafluorophenyl methacrylate)₂₀₀ diblock copolymer nano-objects (10 wt%) via photo-initiated (405 nm irradiation) polymerization-induced self-assembly in DMSO at 37 °C (**M1**), followed by cross-linking reactions using either ethylenediamine or cystamine (**P1** and **P2**, respectively) for transfer into aqueous media.

functional amino compounds, obtaining a series of responsive nanoparticles in high yield.

Herein, functional block copolymer “nano-objects” have been developed via photo-PISA based on poly(ethyleneglycol)₁₁₃-*b*-poly(pentafluorophenyl methacrylate)_x (PEG₁₁₃-*b*-P(PFMA)_x) in DMSO. Block copolymer nanospheres with degree of polymerization, DP_{PFMA} = 200 were used as precursors to prepare responsive nanoparticles (**Scheme 1**). The nanoparticles were stabilized using a disulfide-containing cross-linker to prepare thiol-functional nanospheres that can undergo GSH-triggered disassembly. In the present work, we report the first example of using PFMA as the core-forming block for RAFT-mediated PISA conducted in DMSO. In addition, the reactivity and versatility of the resulting polymeric PPFMA active ester-based platform toward post-polymerization modification with different diamines (ethylenediamine and cystamine) was investigated.

In order to conduct dispersion PISA, conditions should be selected such that the monomer is soluble prior to polymerization. However, as the polymerization progresses, the resulting polymer should undergo a solubility transition and become insoluble. We noted that our initial attempts to prepare PPFMA homopolymers in DMSO via RAFT resulted in macroscopic precipitation. We thus reasoned that as PFMA monomer is readily soluble in DMSO at concentrations in excess of 20 wt%, polymerization of PFMA in DMSO appeared promising for PISA. Alcohols could potentially be used as alternative solvents for PISA of PFMA, but were avoided due to possibility of PFMA alcoholysis and the less toxic nature of DMSO.

To conduct photo-PISA using PFMA, polymerizations were carried out in anhydrous DMSO (≥99.9%) to avoid hydrolysis of the monomer, in the presence of a PEG₁₁₃-mCTA under visible-light irradiation (405 nm). This resulted in the formation of block copolymers that possessed a stabilizing PEG block and an insoluble PPFMA block (Figure S1, Supporting Information). A kinetic experiment for PEG₁₁₃-*b*-P(PFMA)₂₀₀ was conducted to assess the controlled behavior of the polymerization. As shown in Figure S2A, Supporting Information, RAFT polymerization of PFMA in DMSO followed a first-order kinetic profile. Importantly, the kinetic plot exhibited a change in slope at approx. 0.6 h. This characteristic feature of a PISA reaction indicates the onset of self-assembly.^[15] Size-exclusion

chromatography (SEC) analysis of the polymerization revealed bimodal distributions, with two populations assigned to the growing block copolymer and the macro-CTA. At first glance, the vast quantity of unconsumed macro-CTA seemed to suggest that the re-initiation efficiency of the polymerization was poor. However, previous reports of fluorinated block copolymers have attributed this bimodal distribution to overexaggeration of the peak corresponding to the macro-CTA due to the low refractive indices of fluorinated polymers.^[36] The final PEG₁₁₃-*b*-P(PFMA)₂₀₀ copolymer obtained had a $M_n = 63.6 \text{ kg mol}^{-1}$ and $D_M = 1.2$, as determined by SEC analysis (Figure S2B, Supporting Information).

Photo-polymerization of PFMA in DMSO mediated by PEG₁₁₃-mCTA resulted in the formation of nanoparticles via PISA. Nanoparticle formation was evidenced by the onset of turbidity within the polymerization solution. To evaluate the assemblies that arose from the PISA process, the particles were characterized by transmission electron microscopy (TEM), atomic force microscopy (AFM), and light scattering techniques. **Figure 1A**; Figures S3, S4, Supporting Information, demonstrate that PISA in DMSO using DP_{PFMA} = 200 resulted in the formation of spherical particles, **M1**, with an average diameter of 320 nm. The spherical particles were extremely uniform in size (PD = 0.06 from dynamic light scattering [DLS]) and appeared to possess rough surface topologies that were visible by both dry-state TEM and AFM analysis. Estimated parameters for the particles' size distribution (PSD) by DLS were found to be in excellent agreement with those estimated by the construction of a histogram via inspection and counting of particles in the TEM images (Figure 1A). Furthermore, as shown in Table S1 and Figure S4, Supporting Information, the synthesis of PEG₁₁₃-*b*-PPFMA_x block copolymers with different DPs and varying total solids content, solely resulted in the formation of spherical particles of similar characteristics.

SLS analysis for **M1** was used to further confirm the observed particle morphology by exploiting the size of the particles relative to the laser wavelength and the narrow PSD. For the particles in DMSO, analysis of SLS data gave the following estimates: $M_w = 1.1 \pm 0.2 \times 10^9 \text{ Da}$; $R_G z = 139.4 \pm 4.4 \times 10^{-9} \text{ m}$; and $R_H z = 178.1 \pm 7.6 \times 10^{-9} \text{ m}$ (see Supporting Information for further details). In the absence of any further information,

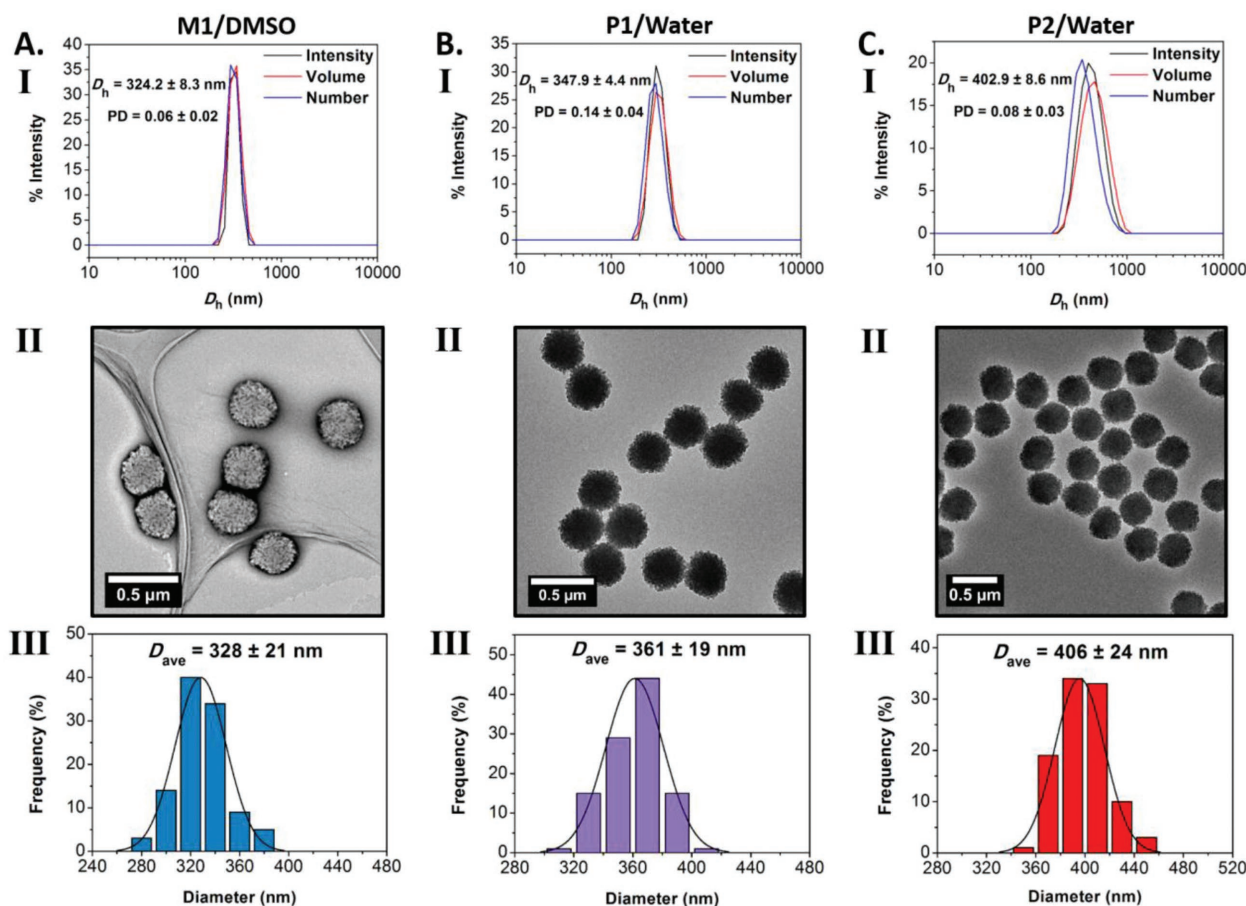


Figure 1. A) PEG₁₁₃-*b*-PPFMA₂₀₀ particles in DMSO (**M1**), B) cross-linked particles using ethylenediamine after transition to DI water (**P1**), and C) cross-linked particles using cystamine after transition to DI water (**P2**). I) Intensity-weighted size distributions of particles obtained by DLS, along with the average D_h and PD values (the error shows the standard deviation from five repeat measurements), II) representative dry-state TEM images of purified particles, stained with 1 wt% uranyl acetate, and III) histograms of particles' size distribution measured from particle analysis from TEM images. In each case, at least 100 particles were analyzed.

the ratio $R_{Gz}/R_{Hz} = 0.783$ would usually be taken to indicate the particles were likely to be homogeneous (the theoretical value is $R_G/R_H = 0.775$). However, given that the empirical estimate was based upon small angle scattering data only, we sought to verify this result using the whole data set by comparison to the theoretical form factor for a spherical particle of this size. Taking into account the assumptions we would make to calculate the form factor and the scale of the error at large angles, we judged that we would be able to differentiate between a homogeneous sphere and a sphere containing an aqueous cavity with confidence. However, despite their capacious size, the SLS data also indicated that the nanoparticles were most likely to be solid spheres with no internal cavity, as shown in Figure S10, Supporting Information. By comparing M_w for the particle to the estimated molecular weight of the polymer, these assemblies were also found to possess large aggregation numbers of $\approx 2 \times 10^4$.

When **M1** particles were transitioned into water via a solvent-switch method aggregation was observed which led to macroscopic precipitation. Given the high glass transition temperature (T_g approx. 125 °C)^[37] and hydrophobicity of

PPFMA, it is unlikely that this aggregation occurs via a unimer exchange mechanism. Therefore, we hypothesized that the particles aggregate via a fusion mechanism, leading to the formation of large particles and subsequent precipitation. To stabilize the particles in H₂O, we adopted a cross-linking strategy which took advantage of the inherent reactivity of the pendent activated esters of PPFMA. Prior to transitioning the particles into H₂O, the polymer solutions were treated with diamines, ethylenediamine (EDA) (**P1**) or cystamine (**P2**), to form amide cross-links in the nanoparticles. Cross-linking was conducted immediately following PISA using 2 eq. of diamine and 4 eq. of triethylamine (TEA) (with respect to PEG₁₁₃-*b*-PPFMA₂₀₀ block copolymer) as a catalyst at 50 °C for 15 h. During this process, amide bond formation occurred via reaction between the cross-linking agents and the activated ester bonds. A cross-linking efficiency of 90% was measured via FTIR spectroscopic analysis for EDA, while a slightly lower cross-linking efficiency of 88% was achieved using cystamine (Figure S6, Supporting Information). FTIR confirmed the absence of pentafluorophenyl ester at 1780 cm⁻¹ (carbonyl group) and the appearance of new signal at 1650 cm⁻¹ that can be attributed to amide bond

formation (C=O). Additionally, due to the presence of TEA, the remaining unreacted pentafluoro esters were hydrolyzed to give poly(methacrylic acid) (Figure S5B, Supporting Information), resulting in the formation of stabilized nanoparticles with partially hydrophilic cores. The hydrolysis reaction was confirmed as a result of the absence of any fluorine signals in the ^{19}F NMR spectrum of the cross-linked particles (Figure S5C, Supporting Information) and the appearance of a new C=O vibration (1755 cm^{-1}) in the IR spectra of both cross-linked samples which could be assigned to the newly formed carboxylic acids (Figure S6, Supporting Information). Cross-linking was also confirmed by DLS analysis in THF, a good solvent for both blocks. Under these conditions, the uncrosslinked **M1** particles dissolved completely into unimers. In contrast, the cross-linked **P1** and **P2** particles remained intact, and possessed an average diameter that was larger than that measured prior to cross-linking due to swelling of the particles by the solvent (Figure S7, Supporting Information).

It is important to note that the cross-linking reactions were conducted on the preformed assemblies, so it was not expected to alter their morphology or aggregation number. Indeed, as confirmed by light scattering, TEM, and AFM analysis (Figures S8 and S9, Supporting Information), the size and morphology of the nanoparticles remained consistent after cross-linking, when using both the permanent EDA and responsive cystamine cross-linkers. Following cross-linking, the nanoparticles were purified by repeated centrifugation/resuspension cycles in DMSO and subsequently H_2O . For two different samples of cross-linked particles in water (**P1** and **P2**), light scattering data was recorded to allow comparison between form factors recorded for the particles before and after cross-linking and solvent-switch and to investigate any internal structural changes occurring over the course of these processes. As shown in Figure S10, Supporting Information, in both cases the resulting estimate for the external radius of the sphere fell within the 95% confidence interval associated with the estimated value in DMSO; again, each sample was judged to be homogeneous spheres and if an aqueous inner cavity was

present then its volume would account for less than 3% of the total particle volume.

Nanoparticles cross-linked with cystamine were proposed to possess redox responsiveness due to the presence of disulfide bonds within the cross-links. Disulfide linkages can be reduced by biologically relevant thiols such as cysteine and GSH. Upon reduction, the responsive particles were expected to break down into their constituent polymers, whilst the non-responsive cross-linked particles were not expected to change. To assess the response of the nanoparticles to a reducing environment, a sample of the two cross-linked purified particles were treated with different concentrations of GSH in PBS buffer. DLS was then employed to monitor the changes in size of the particles over time.

As shown in Figure 2, **P2** nanoparticles containing cystamine cross-links treated with $10\text{ }\mu\text{M}$ GSH remained stable over a period of >5 h. No significant changes in Z-average size or PD were observed during this time. When the particles were exposed to a higher concentration of reducing agent ($[\text{GSH}] = 10\text{ mM}$, concentration similar to the cytoplasmic environment of cancerous cells), a dramatic increase in size and PD was observed that occurred immediately upon treatment with GSH. This size increase corresponds to an initial swelling of the particles; over further time, the particles gradually degraded (Figure 2B inset). Similar behavior has also been reported in the literature.^[6,38] In stark contrast, EDA cross-linked **P1** particles did not respond to either concentration of GSH over the timescale of the experiment, as expected for EDA, which does not contain a disulfide bond therefore, treatment with GSH yielded no apparent response.

Finally, the cytotoxicity of the two cross-linked polymeric nanoparticles was evaluated on A549 cells (human lung cancer fibroblasts). As shown in Figure 3, a viability of >90% was observed for cells incubated with either **P1** or **P2** for 72 h, demonstrating the high cytocompatibility of the materials.

In this work, we report the synthesis of fluorine-containing diblock copolymer “nano-objects” prepared by photo-initiated RAFT PISA in DMSO. A combination of light scattering and

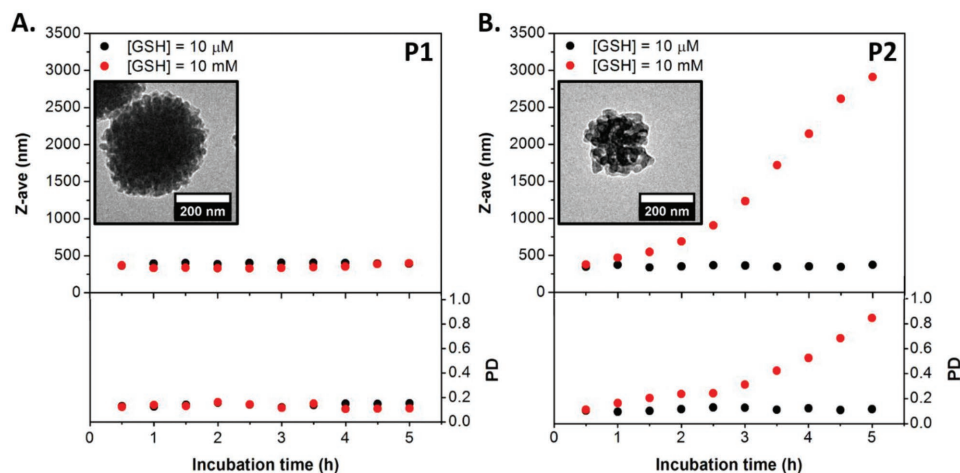


Figure 2. A) Z-Average diameter and PD values of EDA cross-linked **P1** particles as a function of $[\text{GSH}] = 10\text{ }\mu\text{M}$ and 10 mM . B) Z-Average diameter and PD values of cystamine cross-linked **P2** particles as a function of $[\text{GSH}] = 10\text{ }\mu\text{M}$ and 10 mM (insets show dry-state TEM images of **P1** and **P2** after 5 days of treatment with 10 mM GSH).

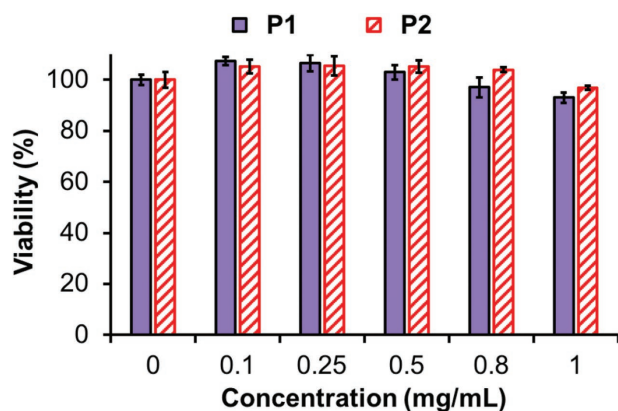


Figure 3. A549 cells viability upon incubation with increasing concentrations of P1 or P2 for 72 h. Viability is expressed as percentage of control (0 mg mL⁻¹ of polymers). Results are expressed as value \pm standard deviation ($n = 3$).

microscopy techniques were used to characterize the resulting morphologies, showing that by varying the DP of the core-forming block of PFMA, only homogenous textured spheres could be obtained. Subsequently, the presence of the pentafluorophenyl ester groups was exploited to attach amino compounds to yield cross-linked polymeric “nano-objects” in aqueous solutions with high efficiency. The morphological characterization of the cross-linked particles also showed that the morphologies were retained after the post-polymerization modification process. Disassembly of the disulfide cross-linked nanoparticles occurred in the presence of intracellular concentrations of GSH. Finally, the cytotoxicity of the cross-linked materials was evaluated in vitro to explore possible biomedical applications of the nanostructures. This method represents a facile and straightforward approach for the generation of new functional and responsive polymers, which may be promising candidates as drug delivery vehicles.

Supporting Information

Supporting Information is available from the Wiley Online Library or from the author.

Acknowledgements

B.C. and P.G.G. contributed equally to this work. The work was supported by the ERC (grant number 615142), EPSRC, and University of Warwick. B.C. acknowledges funding from the European Union's Horizon 2020 research and innovation programme under the Marie Skłodowska-Curie Grant Agreement No. 703934, FluoroDendriNostic project. Mr. B. Li (University of Warwick) is thanked for dry-state TEM assistance and Mr. G. Herwig (University of Birmingham) is thanked for AFM assistance.

Conflict of Interest

The authors declare no conflict of interest.

Keywords

activated esters, nano-objects, polymer functionalization, polymerization-induced self-assembly (PISA), reversible addition–fragmentation chain-transfer polymerization (RAFT)

Received: June 13, 2018

Revised: June 29, 2018

Published online:

- [1] M. Wei, Y. Gao, X. Li, M. J. Serpe, *Polym. Chem.* **2017**, *8*, 127.
- [2] T. Yildirim, I. Yildirim, R. Yañez-Macias, S. Stumpf, C. Fritzsche, S. Hoepfner, C. Guerrero-Sanchez, S. Schubert, U. S. Schubert, *Polym. Chem.* **2017**, *8*, 1328.
- [3] Y. Tao, S. Liu, Y. Zhang, Z. Chi, J. Xu, *Polym. Chem.* **2018**, *9*, 878.
- [4] M. A. Ward, T. K. Georgiou, *Polymers* **2011**, *3*, 1215.
- [5] J. Rosselgong, A. Blanazs, P. Chambon, M. Williams, M. Semsarilar, J. Madsen, G. Battaglia, S. P. Armes, *ACS Macro. Lett.* **2012**, *1*, 1041.
- [6] T. Yildirim, A. Traeger, E. Preussger, S. Stumpf, C. Fritzsche, S. Hoepfner, S. Schubert, U. S. Schubert, *Macromolecules* **2016**, *49*, 3856.
- [7] B. Khorsand, G. Lapointe, C. Brett, J. K. Oh, *Biomacromolecules* **2013**, *14*, 2103.
- [8] M. Gulfam, T. Matini, P. F. Monteiro, R. Riva, H. Collins, K. Spriggs, S. M. Howdle, C. Jérôme, C. Alexander, *Biomater. Sci.* **2017**, *5*, 532.
- [9] J. C. Foster, S. C. Radzinski, X. Zou, C. V. Finkelstein, J. B. Matson, *Mol. Pharm.* **2017**, *14*, 1300.
- [10] J. G. Croissant, Y. Fatieiev, K. Julfakyan, J. Lu, A. H. Emwas, D. H. Anjum, H. Omar, F. Tamanoi, J. I. Zink, N. M. Khashab, *Chem. A Eur. J.* **2016**, *22*, 14806.
- [11] N. Kamaly, B. Yameen, J. Wu, O. C. Farokhzad, *Chem. Rev.* **2016**, *116*, 2602.
- [12] L. Deng, G. Wang, J. Ren, B. Zhang, J. Yan, W. Li, N. M. Khashab, *RSC Adv.* **2012**, *2*, 12909.
- [13] J. F. Quinn, M. R. Whittaker, T. P. Davis, *Polym. Chem.* **2017**, *8*, 97.
- [14] S. L. Canning, G. N. Smith, S. P. Armes, *Macromolecules* **2016**, *49*, 1985.
- [15] A. Blanazs, J. Madsen, G. Battaglia, A. J. Ryan, S. P. Armes, *J. Am. Chem. Soc.* **2011**, *133*, 16581.
- [16] J. Rieger, *Macromol. Rapid Commun.* **2015**, *36*, 1458.
- [17] L. Shen, H. Guo, J. Zheng, X. Wang, Y. Yang, Z. An, *ACS Macro Lett.* **2018**, *7*, 287.
- [18] M. Huo, D. Li, G. Song, J. Zhang, D. Wu, Y. Wei, J. Yuan, *Macromol. Rapid Commun.* **2018**, *39*, 1700840.
- [19] M. Huo, M. Zeng, D. Wu, Y. Wei, J. Yuan, *Polym. Chem.* **2018**, *9*, 912.
- [20] W. Zhao, H. T. Ta, C. Zhang, A. K. Whittaker, *Biomacromolecules* **2017**, *18*, 1145.
- [21] A. Xu, Q. Lu, Z. Huo, J. Ma, B. Geng, U. Azhar, L. Zhang, S. Zhang, *RSC Adv.* **2017**, *7*, 51612.
- [22] E. H. Discekici, A. Anastasaki, R. Kaminker, J. Willenbacher, N. G. Truong, C. Fleischmann, B. Oschmann, D. L. Lunn, J. Read de Alaniz, T. P. Davis, C. M. Bates, C. J. Hawker, *J. Am. Chem. Soc.* **2017**, *139*, 5939.
- [23] B. Xu, Y. Liu, X. Sun, J. Hu, P. Shi, X. Huang, *ACS Appl. Mater. Interfaces* **2017**, *9*, 16517.
- [24] X. Zhang, X. Huang, S. W. Kwok, S. Soh, *Adv. Mater.* **2016**, *28*, 3024.
- [25] P. Theato, *J. Polym. Sci. Part A Polym. Chem.* **2008**, *46*, 6677.
- [26] M. Eberhardt, R. Mruk, R. Zentel, P. Theato, *Eur. Polym. J.* **2005**, *41*, 1569.
- [27] F. D. Jochum, P. Theato, *Macromolecules* **2009**, *42*, 5941.
- [28] Q. Zhang, P. Schattling, P. Theato, R. Hoogenboom, *Eur. Polym. J.* **2015**, *62*, 435.



- [29] H. Gaballa, S. Lin, J. Shang, S. Meier, P. Theato, *Polym. Chem.* **2018**, 9, 3355.
- [30] M. I. Gibson, E. Fröhlich, H. A. Klok, *J. Polym. Sci. Part A Polym. Chem.* **2009**, 47, 4332.
- [31] M. I. Gibson, M. Danial, H. A. Klok, *ACS Comb. Sci.* **2011**, 13, 286.
- [32] L. Nuhn, M. Hirsch, B. Krieg, K. Koykov, K. Fischer, M. Schmidt, M. Helm, R. Zentel, *ACS Nano* **2012**, 6, 2198.
- [33] L. Nuhn, S. Tomcin, K. Miyata, V. Mailänder, K. Landfester, K. Kataoka, R. Zentel, *Biomacromolecules* **2014**, 15, 4111.
- [34] H. Zhao, W. Gu, M. W. Thielke, E. Sterner, T. Tsai, T. P. Russel, E. B. Coughlin, P. Theato, *Macromolecules* **2013**, 46, 5195.
- [35] N. Vanparijs, L. Nuhn, S. J. Paluck, M. Kokkinopoulou, I. Lieberwirth, H. D. Maynard, B. G. De Geest, *Nanomedicine* **2016**, 11, 2631.
- [36] M. Semsarilar, E. R. Jones, S. P. Armes, *Polym. Chem.* **2014**, 5, 195.
- [37] R. Gentsch, F. Pippig, K. Nilles, P. Theato, R. Kikkeri, M. Maglinao, B. Lepenies, P. H. Seeberger, H. G. Börner, *Macromolecules* **2010**, 43, 9239.
- [38] P. Bilalis, S. Varlas, A. Kiafa, A. Velentzas, D. Stravopodis, H. Iatrou, *J. Polym. Sci. Part A Polym. Chem.* **2016**, 54, 1278.